Quantifying Virtual Self-Motion Sensations Induced by Galvanic Vestibular Stimulation

Gallagher, M.[1,2], Romano, F.[3], Bockisch, C.J.[3, 5,6,7,8], Ferrè, E. R.[2,4], & Bertolini, G.[9]

[1] School of Psychology, University of Kent, Canterbury, UK

[2] School of Psychology, Royal Holloway, University of London, Egham, UK

[3] Department of Neurology, University Hospital Zurich, Zurich, Switzerland

[4] Department of Psychological Sciences, Birkbeck University of London, London, UK

[5] Faculty of Medicine, University of Zurich, Zurich, Switzerland

[6] Clinical Neuroscience Center, Zurich, Switzerland

[7] Department of Otorhinolaryngology, University Hospital Zurich, Zurich, Switzerland

[8] Department of Ophthalmology, University Hospital Zurich, Zurich, Switzerland

[9] Institute of Optometry, University of Applied Sciences and Arts Northwestern Switzerland, Olten, Switzerland

Corresponding Author:
Maria Gallagher
School of Psychology,
Keynes College
University of Kent
Canterbury,
CT27NP
m.gallagher@kent.ac.uk

Keywords: Vestibular system; Galvanic Vestibular Stimulation; Natural Vestibular stimulation, vestibular perception

Abstract

Background: The vestibular system provides a comprehensive estimate of self-motion in 3D space. Widely used to artificially stimulate the vestibular system, binaural-bipolar square-wave Galvanic Vestibular Stimulation (GVS) elicits a virtual sensation of roll rotation. Postural responses to GVS have been clearly delineated, however quantifying the perceived virtual rotation vector has not been fully realised.

Objective: We aimed to quantify the perceived virtual roll rotation vector elicited by GVS using a psychophysical approach on a 3D turntable.

Methods: Participants were placed supine on the 3D turntable and rotated around the naso-occipital axis while supine and received square-wave bipolar-binaural GVS or sham stimulation. GVS amplitudes and intensities were systematically manipulated. The turntable motion profile consisted of a velocity step of 20°/s^2 until the trial velocity between 0-20°/s was reached, followed by a 1°/s ramp until the end of the trial. In a psychophysical adaptive staircase procedure, we systematically varied the roll velocity to identify the exact velocity that cancelled the perceived roll sensation induced by GVS.

Results: Participants perceived a virtual roll rotation towards the cathode of approximately 2°/s velocity for 1 mA GVS and 6°/s velocity for 2.5 mA GVS. The observed values were stable across repetitions.

Conclusions: Our results quantify for the first time the perceived virtual roll rotations induced by binaural-bipolar square-wave GVS. Importantly, estimates were based on perceptual judgements, in the absence of motor or postural responses and in a head orientation where the GVS-induced roll sensation did not interact with the perceived direction of gravity. This is an

important step towards applications of GVS in different settings, including sensory substitution or Virtual Reality.

Introduction

Moving through the environment elicits a host of multisensory information regarding the location of the body in 3D space. The visual system detects optic flow from the external world, proprioception signals the position of the body, and vestibular signals provide information regarding acceleration of the head [1]. Vestibular signals are particularly important for self-motion [3,9,10], and the integration of signals from the semi-circular canals and otolith organs provides us with a comprehensive representation of the motion of our head in the three-dimensional (3D) space [7,17]. The vestibular system can be artificially stimulated. A widely used method is Galvanic Vestibular Stimulation (GVS). Electrodes are placed on the mastoids, stimulating the vestibular nerve [8,21,33]. Although debate is still ongoing, it seems likely that GVS affects the vestibular nerve, and therefore stimulates both semicircular canal and otolith afferents [8,21,23,33] (but see [6] for contrasting findings). Often, a bipolar-binaural configuration is used, with anodal currents decreasing vestibular nerve firing rates and cathodal currents increasing them [18]. Different waveforms of stimulation can be used, including stochastic stimulation to increase noise in the vestibular nerves, or square-wave (i.e. step or boxcar) stimulation to elicit virtual sensations of rotation. A wide bilateral cortical network has been shown to be activated by GVS, including the insula, parietal operculum, midcingulate cortex, and somatosensory cortices [12,26,27]. In the past decades, GVS has been largely used to investigate the role of the vestibular system in a range of perceptual and cognitive tasks, including body representation, decision making and visual spatial attention [13,25,28,35].

Postural responses are triggered by GVS when participants are standing [4,14,37]. Wardman, Day and Fitzpatrick (2003) administered 0.3 mA and 0.5 mA of GVS in a boxcar waveform to participants standing upright and measured the postural response during and after eight seconds of stimulation [37]. The GVS postural response was divided into three phases. First, an initial rapid step with an average velocity of 15mm/s^{-1} was seen in the direction of the anode. This phase of the response lasted between 0.4-0.9 seconds after stimulation onset. Next, a constant velocity ramp of approximately 4mm/s^{-1} continued from 1.6-6 seconds after GVS onset. Finally, a rapid movement towards the original starting point with a velocity of approximately 10mm/s^{-1} was seen at 8.4-8.9s after GVS onset (0.4-0.9s after GVS offset). Importantly, stimulation intensity seems to be crucial: GVS at 0.5 mA resulted in a greater displacement than stimulation at 0.3 mA [37]. Interestingly, modifying the position of the head relative to the body can change the postural response elicited by GVS. Cathers et al. (2005) administered 2 mA of boxcar GVS when the head was turned over the shoulder and either upright or pitched downwards [4]. By adopting these head postures, the axis of rotation shifts from a sensation of roll to pitch or yaw respectively in head coordinates. Crucially, while a sensation of pitch requires significant postural adjustments to maintain balance, the sensation in yaw does not. Accordingly, when the head was upright, a large sway response towards the anode was seen at GVS onset, with a return to the original posture on GVS offset. By contrast, when the head was positioned downwards, only small transient responses towards the cathode were seen. Taken together, these results suggest that vestibular inputs from GVS are integrated in function of head position, resulting in altered sensations of motion and appropriate postural responses [4].

But what is the *perceptual* sensation evoked by GVS? It has been consistently reported that binaural-bipolar GVS results in a polarity-dependent virtual roll-rotation vector, where the individual perceives a sense of roll rotation towards the cathode [4,14,15]. It has been proposed that the virtual rotation vector induced by GVS arises as a result of changes in vestibular afferent firing rates mimicking a real motion of the head in space [8,14]. Real head motion stimulates one or more pairs of semicircular canals, generating opposite changes in the firing rates of the respective vestibular afferents. The change in firing rate corresponds to the magnitude of the rotation vector perpendicular to each semicircular canal plane. The signals from the semicircular canals can therefore be vector summed to provide a net rotation vector in skull-fixed coordinates. When the system is stimulated using GVS, the semicircular canal vector depends on GVS intensity, with larger perceived rotation amplitudes with higher GVS intensities [8]. The net GVS-evoked virtual rotation vector is then computed as a vector dot product between gravitational cues regarding the location of the head in space and the semicircular canal vector sum, resulting in a rotation axis estimated to pass 18.8^{o} below Reid's plane [8,14]. Given the angle of the GVS rotation axis, perceived rotation reverses direction when the head is pitched backwards or forwards [8]. Crucially, the previously described postural responses appear to accord with these predictions [4,36].

While neuroimaging and postural effects of GVS have been extensively studied, a detailed quantification of the perceived virtual rotation vector has not yet been achieved. Quantifying the self-motion sensation elicited by GVS is an essential step not only for the theoretical understanding of this technique, but also for potential applications. For example, GVS could be used as a sensory substitution method in patients with bilateral vestibular loss who may benefit from the stimulation to restore lost vestibular function [30,39], as well as provide additional vestibular cues in Virtual Reality (VR) settings [5,32]. Precise estimates of the natural equivalent motion of GVS need to be described for these applications to be effective. Importantly, it is still unknown whether the virtual rotation sensation evoked by GVS is stable across time and multiple exposures. Ertl, Klimek, Boegle, Stephan and Dieterich (2018) found that GVS detection thresholds for binaural-bipolar boxcar stimulation were similar across repeated sessions on different days, which might suggest that the sensations evoked by GVS are similar across different exposures [11]. Whether the virtual rotation percept itself remains robust across time has not been investigated. Here we aimed to quantify the natural equivalent perceived motion of binaural-bipolar boxcar GVS by estimating the point of equivalence between passive natural motion and GVS sensations and investigated its stability over time.

Given previous research [4,8,36], we expected participants to experience a sensation of roll rotation towards the cathode, and we expected no significant difference between repeated sessions.

Methods

Ethics

The experimental protocol was approved by the Canton of Zurich ethics committee. The study was conducted in line with the Declaration of Helsinki. Written informed consent was obtained from participants prior to commencing the study.

Participants

Eight participants (three female, mean age = 34.38, SD = 12.34) completed our psychophysical study, including authors M.G., G.B., F.R. and C.B.. Six participants were right-handed according to their Edinburgh Handedness Inventory [29] scores, while the remaining two were left-handed. Exclusion criteria were any history of neurological, psychiatric, or vestibular conditions, epilepsy or family history of epilepsy. All participants' data was included in the final analysis, resulting in a total sample size of eight participants.

Procedure

After completing informed consent procedures, participants were given task instructions. Here we attempted to find the physical rotation stimulus that precisely cancelled the percept evoked by GVS. Participants were secured on a human 3D-Turntable at University of Zurich, Department of Neurology, positioned so that the centre of the head was at the intersection of the three rotation axes. A response bar and button were fixed just in front of the participants' hands. At the beginning of the experiment, the turntable was rotated such that the participants were supine during the experiment. This posture was chosen to minimise confounds of position change with respect to gravity during the trials. The experiment consisted of trials where physical motion stimuli were delivered by rotating the turntable clockwise and anticlockwise around an Earth vertical axis passing through the centre of the head. These stimuli elicited a roll sensation to the left and right respectively.

The motion profile of the turntable in each trial consisted of a "velocity step" followed by a ramp to counteract semicircular canal adaptation, and to mimic GVS sensations as closely as possible [36,37]. For the steps, the 3D-Turntable moved with an initial acceleration of 20°/s^2 until the trial velocity was achieved. Potential trial velocities could range from 0-±20°/s in 0.5°/s steps. The turntable continued to accelerate steadily at 1°/s/s (ramp) until the end of the trial (i.e. once a response had been provided or after 5 seconds). An example velocity, acceleration, and position plot can be seen in Figure 2. Once the turntable stopped rotating, the participants were instructed to commence the next trial only once all sensations of rotation had subsided. A minimum break of two seconds was enforced between trials. The experiment was conducted in darkness, so no visual cues for rotation were available. In addition, padding was placed around the participants' legs, to minimise somatosensory cues during rotation.

GVS was administered by a commercial stimulator (Good Vibrations Engineering Ltd., Nobleton, ON, Canada). Electrodes measuring approximately 4cm^2 were coated with NaCl electrode gel and placed on the mastoids (GVS) or on the base of the neck (Sham), approximately located at the C7 vertebral bone. Left-anodal/right-cathodal (L-GVS) stimulation was applied for clockwise trials while right-anodal/left-cathodal (R-GVS) stimulation was applied for anticlockwise trials. As GVS induces a sensation of rotation towards the cathodal side, the stimulation therefore induced a rotation sensation in the opposite direction to the rotation of the 3D-Turntable – for example, L-GVS induces a perception of anticlockwise roll rotation (towards the right ear), and was therefore combined with clockwise (towards the left ear) turntable rotation (Figure 1A). GVS was administered at two different intensities. Both rotation staircases included both polarities of GVS in a boxcar waveform of 5.5 seconds duration, with separate blocks of 1 mA and 2.5 mA.

A sham stimulation condition was also used to control for non-specific sensations, in which stimulation was applied via the electrodes placed on the base of the neck. This stimulation therefore elicits similar cutaneous sensations as GVS without subsequent activation of the vestibular nerve, resulting in no sensations of rotation. This type of stimulation may also control for the participants' idea that an unusual stimulation is occurring, accounting for cognitive factors. Sham stimulation was 2.5 mA, 5.5 seconds duration, and also delivered in left-anodal/right-cathodal (L-Sham) and right-anodal/left-cathodal (R-Sham) polarities according to the direction of 3D-Turntable rotation. Sham at 2.5 mA was chosen to control for the highest intensity of GVS used in the active stimulation conditions.

The QUEST+ algorithm was used to select trial velocities [38]. QUEST+ is a Bayesian adaptive method in which psychometric function parameters are estimated after each trial and next stimulus values are selected. Prior probability distributions for each parameter are first specified, determining the initial stimulus velocity to be presented to the participant. Following each trial, best fitting estimates of the psychometric function parameters are determined from the resulting posterior distribution based on previous responses and stimulus velocities. The next trial velocity is selected based on the value which minimises expected entropy. Testing is stopped when entropy is minimised.

Participants pressed a button to start each trial. Once the button was pressed, the turntable started to move according to the velocity selected by the QUEST+ algorithm [38] and the GVS/Sham stimulation was triggered. Two seconds after the turntable had reached the selected velocity, a beep was sounded to indicate that the participants should report their perceived direction of rotation by rotating the bar clockwise or anticlockwise. Approximately 50 trials were used for both clockwise and anticlockwise staircases, depending on minimum entropy. The staircases were interleaved within each block, resulting in approximately 100 trials per block.

Participants completed four sessions on different days, separated by four days to one week. In each session, all participants first completed the baseline block with sham stimulation, while 1 mA and 2.5 mA GVS conditions were counterbalanced across participants and sessions such that each participant completed each order (i.e., 1 mA or 2.5 mA first) twice across their four sessions. A practice block of 10 trials was completed by all participants before the first session.

Data Analysis

Data from each staircase were fitted with cumulative normal psychometric functions in MATLAB r2017a. The point of subjective equality (PSE) indicated the velocity at which GVS and turntable rotation sensations were cancelled, and was given by the velocity corresponding to 50% ‘clockwise’ responses. Positive PSE values corresponded to a perceived anticlockwise rotation of the head (i.e., a clockwise chair rotation was necessary to cancel the illusory motion), while negative values corresponded to a perceived clockwise rotation of the head. The Just Noticeable Difference (JND) indicated the participants’ precision, and was given by the standard deviation of the psychometric function. The standard deviation is calculated as the inverse of the slope of the cumulative normal psychometric function [22]. Lower JNDs indicated greater precision. An example psychometric function and staircase progression can be seen in Figure 3.

PSEs and JNDs were calculated for each participant, GVS amplitude, and session. Data which was ±2 median absolute deviations from each participants’ median PSE and/or JND was excluded. PSEs and JNDs were fitted with linear mixed effects models in R with lme4 [2,31]. GVS Amplitude and Sessions were fixed factors and Participant was a random factor. Likelihood ratio tests with and without the fixed effects in question were used to obtain *p* values.

Results

Point of Subjective Equality

Overall means and standard errors of PSE values between Sham stimulation and both GVS amplitudes can be seen in Figure 1B. As expected, descriptive statistics showed that Sham stimulation elicited no motion sensations, with values close to 0. Importantly, GVS elicited a sensation of roll rotation towards the side of the cathode, as expected from previous research [4,15]. Moreover, the PSE increased with higher amplitudes of GVS, such that higher velocities of natural vestibular stimulation were required to cancel the GVS sensations.

The best-fitting linear mixed effects model for PSE values during L-GVS was one including only GVS Amplitude as a fixed factor (AIC = 352.12; $X^2(2) = 42.24$, $p < .001$). The intercept for this model (i.e., the motion sensation induced by Sham stimulation) was 0.33°/s ± 0.88 (SE). 1 mA GVS increased the PSE by 1.60°/s ± 0.78 (SE) from Sham values on average, while 2.5 mA GVS increased the PSE from Sham on average by 5.83 °/s ± 0.76 (SE). The random effect of Participant had a variance of 3.93.

Similar effects were seen on PSE values for R-GVS (AIC = 320.83; $X^2(2) = 55.91$, $p < .001$). For this polarity, the intercept was -0.22°/s ± 0.64 (SE), with 1 mA GVS decreasing PSE estimates from Sham values on average by -1.23 °/s ± 0.69 (SE), and 2.5 mA decreased the PSE from Sham on average by -6.41 °/s ± 0.68 (SE). The random effect of Participant had a variance of 1.50.

Neither model including Session as a fixed factor was significantly better at predicting thresholds than the GVS Amplitude only model ($p > .05$). PSEs for L-GVS and R-GVS across each session can be seen in Table 1. Summary statistics (means and SDs averaged across the four sessions) for each participant can be seen in Table 2. Interestingly, PSEs varied considerably across participants, suggesting high individual variability in GVS perception across individuals. Importantly, however, all participants showed the same increase in PSE value with higher amplitudes of stimulation, despite general variability across individuals. Accordingly, the individual differences are likely to result from genuine differences in the perceptual experience of GVS, as opposed to methodological differences, such as electrode placement.

Just Noticeable Difference

Means and standard errors for JNDs between Sham and both GVS amplitudes can be seen in Figure 1C. Descriptive statistics showed that precision decreased with GVS vs Sham stimulation, with decreased precision also with increasing amplitudes of GVS.

The best-fitting linear mixed effects model for JNDs during L-GVS was one including only GVS Amplitude as a fixed factor (AIC = 278.00; $X^2(2) = 34.11$, $p < .001$). The intercept (i.e., precision during Sham stimulation) was 1.09°/s ± 0.49 (SE). 1 mA GVS increased JNDs from Sham on average by 1.01 ± 0.46 (SE), while 2.5 mA GVS increased JNDs from Sham by 3.00 ± 0.45 (SE) on average. The random effect of Participant had a variance of 1.12.

Similar effects were seen for R-GVS (AIC = 324.06; $X^2(2) = 32.92$, $p < .001$). For this polarity, the intercept was 1.11°/s ± 0.69 (SE). 1 mA GVS increased JNDs from Sham on average by 0.63 ± 0.70 (SE), while 2.5 mA increased JNDs from Sham by 4.31 ± 0.69 (SE) on average. The random effect of Participant had a variance of 1.95.

Neither model including Session as a fixed factor was significantly better at predicting JNDs than the GVS Amplitude only model ($p > .05$). JNDs for L-GVS and R-GVS across each session can be seen in Table 3. Summary statistics (means and SDs averaged across the four sessions) for each participant can be seen in Table 4.

Discussion

GVS has been widely used in research to investigate the role of vestibular afferents in postural control, perception, and cognition [13,25,28,35]. Although previous research has systematically quantified the postural responses elicited by GVS [4,36,37], precise estimates of the *perceived* virtual rotation vector have not been fully described. In the present study, for the first time, we estimated the point of equality between GVS-induced virtual rotation and natural rotation. In addition, we also demonstrated that the GVS-induced virtual rotation was stable across repeated exposures. Our finding corroborates previous accounts [4,8,14,37], as both GVS at both 1 mA and 2.5 mA induced a virtual roll-rotation towards the cathode. The direct quantification of the perceived virtual rotation vector allowed us to demonstrate how it increased with higher amplitudes of GVS. Namely, GVS elicited a virtual roll rotation vector of approximately 2^{o}/s velocity for 1 mA stimulation and 6^{o}/s velocity for 2.5 mA stimulation.

Our findings suggest that the percept induced by GVS does not increase simply as a result of increased arousal or attention to the stimulation. Rather, the virtual rotation vector occurs as a direct result of changes in afferent modulation. This finding has very important consequences for the use of GVS, as it confirms that it can be used to induce reliable vestibular-driven illusory self-motion sensations in the absence of other sensory signals. Furthermore, the present study also quantitatively shows which intensity of GVS should be used to induce vestibular-driven self-motion sensations, how reliable the effect is across repetitions, and provides a glimpse into how much it may vary across individuals. Such direct evidence was not available from previous studies that have investigated the GVS virtual rotation vector indirectly through examining postural responses to the stimulation [4,8,14,36,37].

We used a boxcar GVS waveform, with stimulation rapidly reaching its target amplitude, remaining at this intensity for 5.5s, before a rapid offset. In contrast, the rotating chair was moved using a velocity step of 20°/s acceleration until the target velocity was reached, and continued with a 1°/s ramp until the end of the trial. This rotation profile was chosen to avoid semicircular canal adaptation and to mimic previously-reported GVS postural responses [36]. However, consequently the rotating chair could not reach its target velocity as quickly as the GVS reached its target intensity, potentially limiting the amount of rotation cancellation during each individual trial. To mitigate this impact, we asked participants to report their rotation direction ~2s after target chair velocity had been reached, avoiding any potentially confusing sensations during the initial rotation and GVS onset. Importantly, no participants reported difficulty in determining rotation direction at this point in the trial, suggesting that differences in GVS and natural rotation onset had stabilised by the time of response.

Moreover, in the present experiment we attempted to couple physical rotations from the chair with virtual rotations from the GVS as closely as possible. As the rotation induced by GVS is theorised to be through an axis passing 18.8° below Reid's Plane [8,14], the axis of rotation on the turntable was aligned with the centre of the head. Given the complexity of combined and conflicting rotation stimuli, and the uncertainty surrounding the percept induced by GVS, we cannot exclude that the final combined rotation percept was more complex, and may not necessarily be centred on the head [20]. In the present experiment, we believe that our psychophysical task enabled us to ascertain whether participants perceived any residual rotation and accordingly the Point of Subjective Equality is likely a reliable estimate of the

GVS equivalent of physical rotation. However, future research should explore the possibility of combining different rotation axes and how they accord with virtual rotation induced by GVS.

Considerable variability across individual PSEs emerged in our data, suggesting participants differed in their subjective experience of GVS. Importantly, all participants showed an increase in the velocity required to cancel higher intensities of GVS, suggesting that the initial variability is due to individual sensitivity to stimulation, as opposed to methodological issues such as electrode placement. Accordingly, future applications of GVS will require calibration to the individual.

Here we considered roll motion while participants were supine. This posture was chosen to avoid participants utilising additional postural cues with respect to gravity as the 3D turntable moved. The integration of both semicircular canal and otolith cues is vital for accurately estimating self-motion. In particular, inertial acceleration from both tilting the head relative to gravity and linear translation produces an identical response at the otoliths [1,16,19]. Thus, semicircular canal cues must be integrated with otolith cues to distinguish between tilt and translation. Importantly, an internal model of the effects of rotation is used to predict the otolith response, and discrepancies are interpreted as due to linear acceleration [24]. Thus, if a roll rotation signal from the canals during GVS with the head upright occurs, the lack of a signal from the otoliths indicating head tilt relative to gravity is interpreted as meaning the head is simultaneously undergoing interaural translation. Thus, the perceived motion varies as a function of the position of the head with respect to gravity [8]. However, when supine only dynamic angular acceleration cues can be used to estimate self-motion in the coronal plane of the body [34]. As such, further research could therefore investigate whether similar equivalent velocities are elicited from rotation on other axes with respect to gravity. Previous studies have focused on the postural effects of GVS have frequently applied stimulation while the head is tilted forwards, therefore eliciting a sensation of whole-body yaw, rather than head roll [4,8].

In this position, smaller postural responses are elicited, potentially due to lower demands for maintaining balance in comparison to a roll rotation of the head [4]. It may therefore be interesting to explore whether the velocity of the virtual rotation is similar or attenuated when participants perceive body yaw by tilting the head during GVS.

In the past few decades, several studies have considered the effect of GVS on behaviour, and have clearly mapped postural and neuroimaging responses [4,8,12,14,26,27,36,37]. However, no studies have precisely quantified the perceived virtual rotation induced by the artificial vestibular stimulation. Our results suggest that GVS induces a perception of roll rotation towards the cathode, with a velocity ranging from ~1-10°/s across individuals, increasing with higher intensities, and stable within individuals across time.

Acknowledgements:

This work was supported by an Experimental Psychology Society Study Visit Grant and ESRC Overseas Institutional Visit Grant awarded to M.G.. M.G. was also further supported by an ESRC-DTC studentship.

Conflict of interest statement:

The authors declare no conflicts of interest regarding this work.

Author contributions:

M.G., F.R., and C.J.B. performed experiments; M.G. analysed data; E.R.F., G.B. and M.G. conception and design of research; All authors interpreted results of experiments; E.R.F., G.B., C.J.B., and M.G. edited and revised manuscript; all authors approved final version of manuscript.

Data accessibility:

Data are available online at:

https://osf.io/twxn5/?view_only=235d25ec0e644dd09da22624d2464bcd

References

[1] D.E. Angelaki, M.Q. McHenry, J.D. Dickman, S.D. Newlands, and B.J.M. Hess, Computation of Inertial Motion: Neural Strategies to Resolve Ambiguous Otolith Information, *J Neurosci* **19** (1999), 316–327.

[2] D. Bates, M. Mächler, B. Bolker, and S. Walker, Fitting Linear Mixed-Effects Models Using lme4, *Journal of Statistical Software* **67** (2015), 1–48.

[3] K.H. Britten, Mechanisms of Self-Motion Perception, *Annu Rev Neurosci* **31** (2008), 389–410.

[4] I. Cathers, B.L. Day, and R.C. Fitzpatrick, Otolith and canal reflexes in human standing: Vestibular reflexes during standing, *The Journal of Physiology* **563** (2005), 229–234.

[5] M.J. Cevette, J. Stepanek, D. Cocco, A.M. Galea, G.N. Pradhan, L.S. Wagner, S.R. Oakley, B.E. Smith, D.A. Zapala, and K.H. Brookler, Oculo-Vestibular Recoupling Using Galvanic Vestibular Stimulation to Mitigate Simulator Sickness, *Aviation, Space, and Environmental Medicine* **83** (2012), 549–555.

[6] B. Cohen, S.B. Yakushin, and G.R. Holstein, What Does Galvanic Vestibular Stimulation Actually Activate?, *Front Neur* **2** (2012).

[7] K.E. Cullen, Vestibular processing during natural self-motion: implications for perception and action, *Nat Rev Neurosci* **20** (2019), 346–363.

[8] B.L. Day and R.C. Fitzpatrick, Virtual head rotation reveals a process of route reconstruction from human vestibular signals: Perceiving self motion, *The Journal of Physiology* **567** (2005), 591–597.

[9] G.C. DeAngelis and D.E. Angelaki, Visual–Vestibular Integration for Self-Motion Perception, in: : The Neural Bases of Multisensory Processes, M.M. Murray and M.T. Wallace (Eds.), CRC Press/Taylor & Francis, Boca Raton (FL), 2012, p. 21.

[10] J. Dichgans and T. Brandt, Visual-Vestibular Interaction: Effects on Self-Motion Perception and Postural Control, in: : Perception, H. Autrum, R. Jung, W.R. Lowenstein, D.M. MacKay, and H.L. Teuber (Eds.), Springer, Berlin, Heidelberg, 1978, pp. 755–804.

[11] M. Ertl, M. Klimek, R. Boegle, T. Stephan, and M. Dieterich, Vestibular perception thresholds tested by galvanic vestibular stimulation, *J Neurol* **265** (2018), 54–56.

[12] P. zu Eulenburg, S. Caspers, C. Roski, and S.B. Eickhoff, Meta-analytical definition and functional connectivity of the human vestibular cortex, *NeuroImage* **60** (2012), 162–169.

[13] E.R. Ferrè, E. Berlot, and P. Haggard, Vestibular contributions to a right-hemisphere network for bodily awareness: Combining galvanic vestibular stimulation and the "Rubber Hand Illusion," *Neuropsychologia* **69** (2015), 140–147.

[14] R.C. Fitzpatrick and B.L. Day, Probing the human vestibular system with galvanic stimulation, *Journal of Applied Physiology* **96** (2004), 2301–2316.

[15] R.C. Fitzpatrick, J. Marsden, S.R. Lord, and B.L. Day, Galvanic vestibular stimulation evokes sensations of body rotation:, *NeuroReport* **13** (2002), 2379–2383.

[16] S. Glasauer, Interaction of Semicircular Canals and Otoliths in the Processing Structure of the Subjective Zenith, *Ann NY Acad Sci* **656** (1992), 847–849.

[17] J.C. Glover, Vestibular System, in: : Encyclopedia of Neuroscience, Elsevier, 2004, pp. 127–132.

[18] M. Goldberg, E. Smith, and C. Fernandez, Relation Between Discharge Regularity and Responses to Externally Applied Galvanic Currents in Vestibular Nerve Afferents of the Squirrel Monkey, *Journal of Neurophysiology* **51** (n.d.), 1236–1256.

[19] A.M. Green and D.E. Angelaki, Multisensory integration: resolving sensory ambiguities to build novel representations, *Current Opinion in Neurobiology* **20** (2010), 353–360.

[20] J.E. Holly and G. McCollum, Constructive perception of self-motion, *VES* **18** (2009), 249–266.

[21] J. Kim, Head movements suggest canal and otolith projections are activated during galvanic vestibular stimulation, *Neuroscience* **253** (2013), 416–425.
[22] F.A.A. Kingdom and N. Prins, Psychophysics: a practical introduction, Second edition, Elsevier/Academic Press, Amsterdam, 2016.
[23] A. Kwan, P.A. Forbes, D.E. Mitchell, J.-S. Blouin, and K.E. Cullen, Neural substrates, dynamics and thresholds of galvanic vestibular stimulation in the behaving primate, *Nat Commun* **10** (2019), 1904.
[24] J. Laurens and D.E. Angelaki, The functional significance of velocity storage and its dependence on gravity, *Exp Brain Res* **210** (2011), 407–422.
[25] J.-C. Lepecq, C. De Waele, S. Mertz-Josse, C. Teyssèdre, P.T.B. Huy, P.-M. Baudonnière, and P.-P. Vidal, Galvanic Vestibular Stimulation Modifies Vection Paths in Healthy Subjects, *Journal of Neurophysiology* **95** (2006), 3199–3207.
[26] E. Lobel, J.F. Kleine, D.L. Bihan, A. Leroy-Willig, and A. Berthoz, Functional MRI of Galvanic Vestibular Stimulation, *Journal of Neurophysiology* **80** (1998), 2699–2709.
[27] C. Lopez, O. Blanke, and F.W. Mast, The human vestibular cortex revealed by coordinate-based activation likelihood estimation meta-analysis, *Neuroscience* **212** (2012), 159–179.
[28] F.W. Mast, Vestibular Influences on Cognition, in: : Encyclopedia of Neuroscience, Elsevier, 2009, pp. 121–125.
[29] R.C. Oldfield, The assessment and analysis of handedness: The Edinburgh inventory, *Neuropsychologia* **9** (1971), 97–113.
[30] R.J. Peterka, Use of galvanic vestibular feedback for a balance prosthesis, in: : 2012 Annual International Conference of the IEEE Engineering in Medicine and Biology Society, IEEE, San Diego, CA, 2012, pp. 6137–6140.
[31] R Core Team, R: A language and environment for statistical computing, (2022).
[32] R.J. Reed-Jones, J.G. Reed-Jones, L.M. Trick, and L.A. Vallis, Can Galvanic Vestibular Stimulation Reduce Simulator Adaptation Syndrome?, in: : Proceedings of the 4th International Driving Symposium on Human Factors in Driver Assessment, Training, and Vehicle, University of Iowa, Stevenson, Washington, USA, 2007, pp. 534–540.
[33] T. Stephan, A. Deutschländer, A. Nolte, E. Schneider, M. Wiesmann, T. Brandt, and M. Dieterich, Functional MRI of galvanic vestibular stimulation with alternating currents at different frequencies, *NeuroImage* **26** (2005), 721–732.
[34] V.P. Vimal, P. DiZio, and J.R. Lackner, Learning dynamic balancing in the roll plane with and without gravitational cues, *Exp Brain Res* **235** (2017), 3495–3503.
[35] K. Volkening, J. Bergmann, I. Keller, M. Wuehr, F. Müller, and K. Jahn, Verticality perception during and after galvanic vestibular stimulation, *Neuroscience Letters* **581** (2014), 75–79.
[36] D.L. Wardman, B.L. Day, and R.C. Fitzpatrick, Position and velocity responses to galvanic vestibular stimulation in human subjects during standing, *The Journal of Physiology* **547** (2003), 293–299.
[37] D.L. Wardman, J.L. Taylor, and R.C. Fitzpatrick, Effects of galvanic vestibular stimulation on human posture and perception while standing, *The Journal of Physiology* **551** (2003), 1033–1042.
[38] A.B. Watson, QUEST+: A general multidimensional Bayesian adaptive psychometric method, *Journal of Vision* **17** (2017), 10.
[39] M. Wuehr, J. Decker, and R. Schniepp, Noisy galvanic vestibular stimulation: an emerging treatment option for bilateral vestibulopathy, *J Neurol* **264** (2017), 81–86.

Table 1. Mean (SD) PSEs across GVS amplitudes, polarities, and experiment sessions.

	Sham		1 mA		2.5 mA	
Session	**L-Sham**	**R-Sham**	**L-GVS**	**R-GVS**	**L-GVS**	**R-GVS**
1	0.74 (0.89)	-0.48 (0.67)	2.82 (3.08)	-1.03 (0.79)	7.63 (7.51)	-7.42 (3.86)
2	0.44 (0.46)	0.11 (0.43)	2.27 (2.93)	-1.56 (0.77)	6.02 (5.53)	-5.17 (4.81)
3	0.07 (0.35)	-0.30 (0.41)	1.81 (1.34)	-1.49 (1.07)	4.67 (2.94)	-7.73 (5.66)
4	0.28 (0.17)	-0.54 (0.87)	1.09 (0.58)	-1.87 (1.11)	4.74 (4.13)	-4.37 (3.46)

Table 2. Mean (SD) PSEs averaged across sessions for each Participant, GVS Polarity and Amplitude.

	Sham		1 mA		2.5 mA	
Participant	**L-Sham**	**R-Sham**	**L-GVS**	**R-GVS**	**L-GVS**	**R-GVS**
1	0.31 (0.29)	0.13 (0.23)	2.94 (0.53)	-0.87 (0.13)	5.85 (0.01)	-8.92 (1.12)
2	0.31 (0.13)	-0.29 (0.23)	0.87 (0.03)	-1.00 (0.15)	2.94 (1.45)	-4.88 (6.41)
3	-0.04 (0.19)	-0.50 (0.08)	1.15 (0.24)	-2.10 (0.09)	3.54 (1.54)	-7.52 (0.59)
4	0.69 (0.31)	-1.06 (1.53)	2.94 (0.11)	-2.54 (0.17)	10.81 (0.11)	-10.27 (0.21)
5	0.16 (0.01)	0.06 (0.12)	1.39 (0.23)	-0.40 (0.20)	2.85 (1.24)	-2.33 (0.82)
6	0.42 (0.17)	0.06 (0.12)	0.83 (0.08)	-0.20 (0.09)	4.73 (1.74)	-4.23 (1.17)
7	0.25 (0.53)	-0.77 (0.27)	0.13 (0.47)	-2.31 (0.70)	2.84 (1.49)	-3.9 (0.99)
8	0.60 (1.27)	-0.31 (0.35)	5.43 (3.33)	-2.20 (0.51)	19.94 (4.53)	-13.56 (4.06)

Table 3. Mean (SD) JNDs across GVS amplitudes, polarities, and experiment sessions.

	Sham		1 mA		2.5 mA	
Session	**L-Sham**	**R-Sham**	**L-GVS**	**R-GVS**	**L-GVS**	**R-GVS**
1	1.21 (0.17)	1.59 (1.65)	2.65 (2.4)	2.26 (2.06)	5.23 (3.29)	4.49 (4.25)
2	1.24 (0.63)	1.72 (1.48)	2.43 (1.59)	2.00 (1.08)	3.56 (2.27)	6.49 (5.49)
3	0.79 (0.33)	0.76 (0.33)	1.97 (1.39)	1.66 (0.63)	3.57 (3.26)	6.53 (5.14)
4	0.70 (0.21)	0.95 (0.93)	1.51 (0.4)	1.55 (1.00)	2.86 (1.45)	3.29 (1.91)

Table 4. Mean (SD) JNDs averaged across sessions for each Participant, GVS Polarity and Amplitude.

	Sham		1 mA		2.5 mA	
Participant	**L-Sham**	**R-Sham**	**L-GVS**	**R-GVS**	**L-GVS**	**R-GVS**
1	0.99 (0.07)	0.84 (0.43)	3.19 (0.24)	1.50 (1.48)	7.77 (0.54)	4.89 (0.83)
2	1.12 (0.01)	0.56 (0.13)	1.19 (0.11)	2.21 (0.65)	3.34 (1.45)	15.08 (1.69)
3	0.85 (0.15)	0.69 (0.08)	1.50 (0.46)	1.45 (0.08)	1.63 (0.66)	2.22 (0.23)
4	1.31 (0.74)	3.13 (0.31)	1.82 (0.44)	1.53 (1.07)	1.87 (0.20)	2.34 (0.09)
5	0.51 (0.02)	0.45 (0.20)	2.37 (1.25)	0.64 (0.23)	8.07 (2.35)	3.58 (1.28)
6	0.83 (0.44)	0.35 (0.12)	0.61 (0.07)	0.80 (0.48)	1.91 (0.41)	2.40 (0.50)
7	0.92 (0.80)	0.88 (0.28)	1.57 (0.75)	2.66 (0.37)	2.87 (1.16)	2.89 (2.37)
8	1.01 (0.34)	2.37 (1.87)	4.11 (2.66)	3.26 (1.95)	7.40 (0.86)	8.38 (1.21)

Fig. 1. Experiment set up and results. A) 3D turntable and GVS configuration. GVS always elicited virtual rotation in the opposite direction to the physical rotation. B) PSE results across GVS amplitudes and polarities. Bars represent the mean, error bars represent standard error. Points represent individual participants. C) JNDs across GVS amplitudes and polarities. Bars represent the mean, error bars represent standard error. Points represent individual participants.

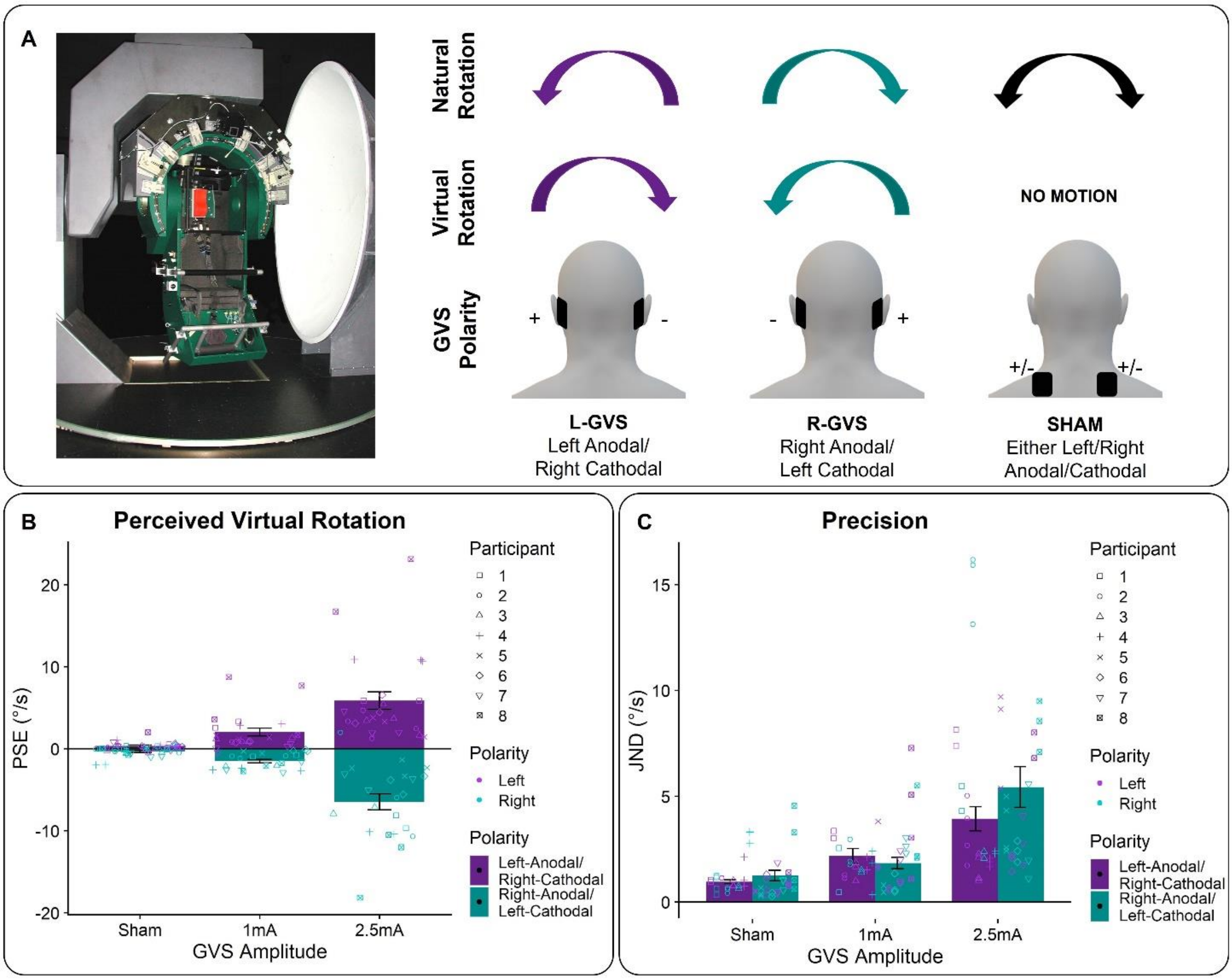
A
Natural Rotation
Virtual Rotation
GVS Polarity
NO MOTION
+
-
+/-
L-GVS
Left Anodal/
Right Cathodal
R-GVS
Right Anodal/
Left Cathodal
SHAM
Either Left/Right
Anodal/Cathodal
B
Perceived Virtual Rotation
PSE (°/s)
GVS Amplitude
Sham
1mA
2.5mA
Participant
Polarity
Left
Right
Left-Anodal/
Right-Cathodal
Right-Anodal/
Left-Cathodal
C
Precision
JND (°/s)

Fig 2. Example velocity, acceleration, position plot for a 20°/s velocity trial.

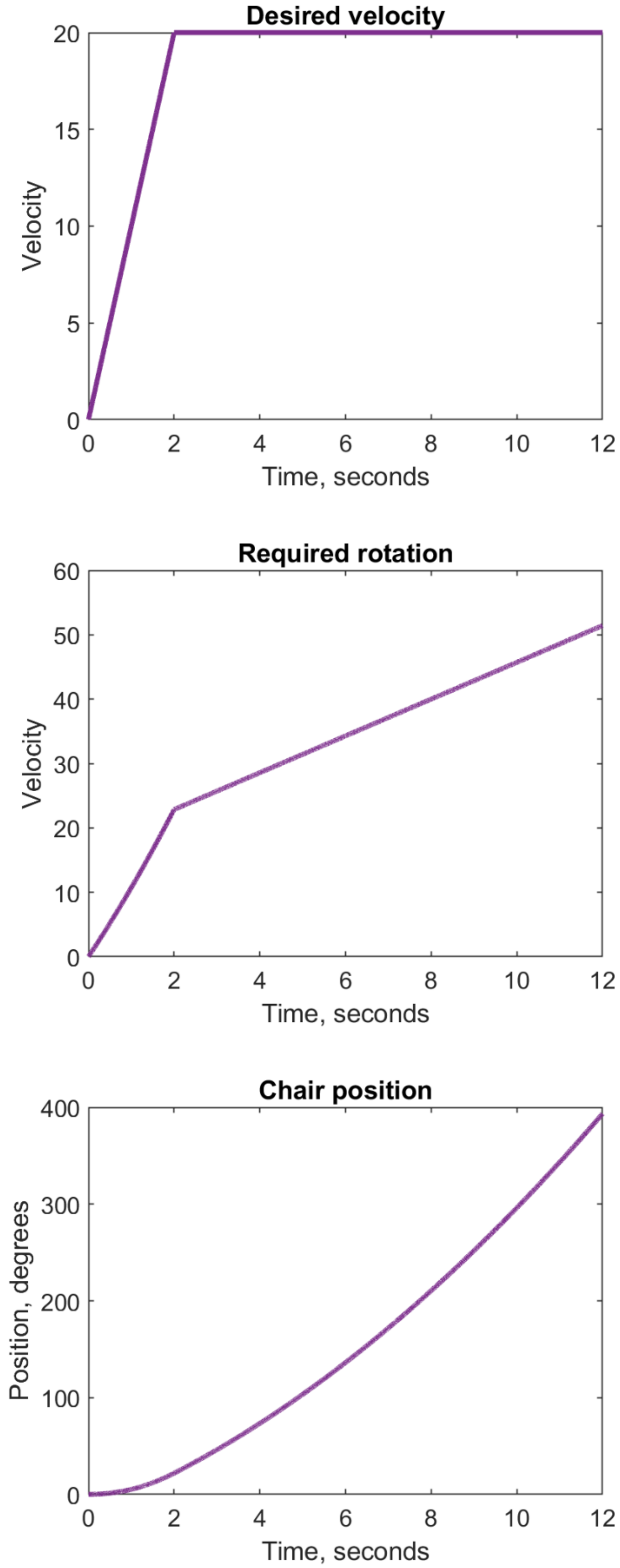
Desired velocity
Velocity
0
5
10
15
20
Time, seconds
0
2
4
6
8
10
12
Required rotation
Velocity
0
10
20
30
40
50
60
Time, seconds
0
2
4
6
8
10
12
Chair position
Position, degrees
0
100
200
300
400
Time, seconds
0
2
4
6
8
10
12

Fig. 3. A) Example individual psychometric functions. B) Example staircase evolution.

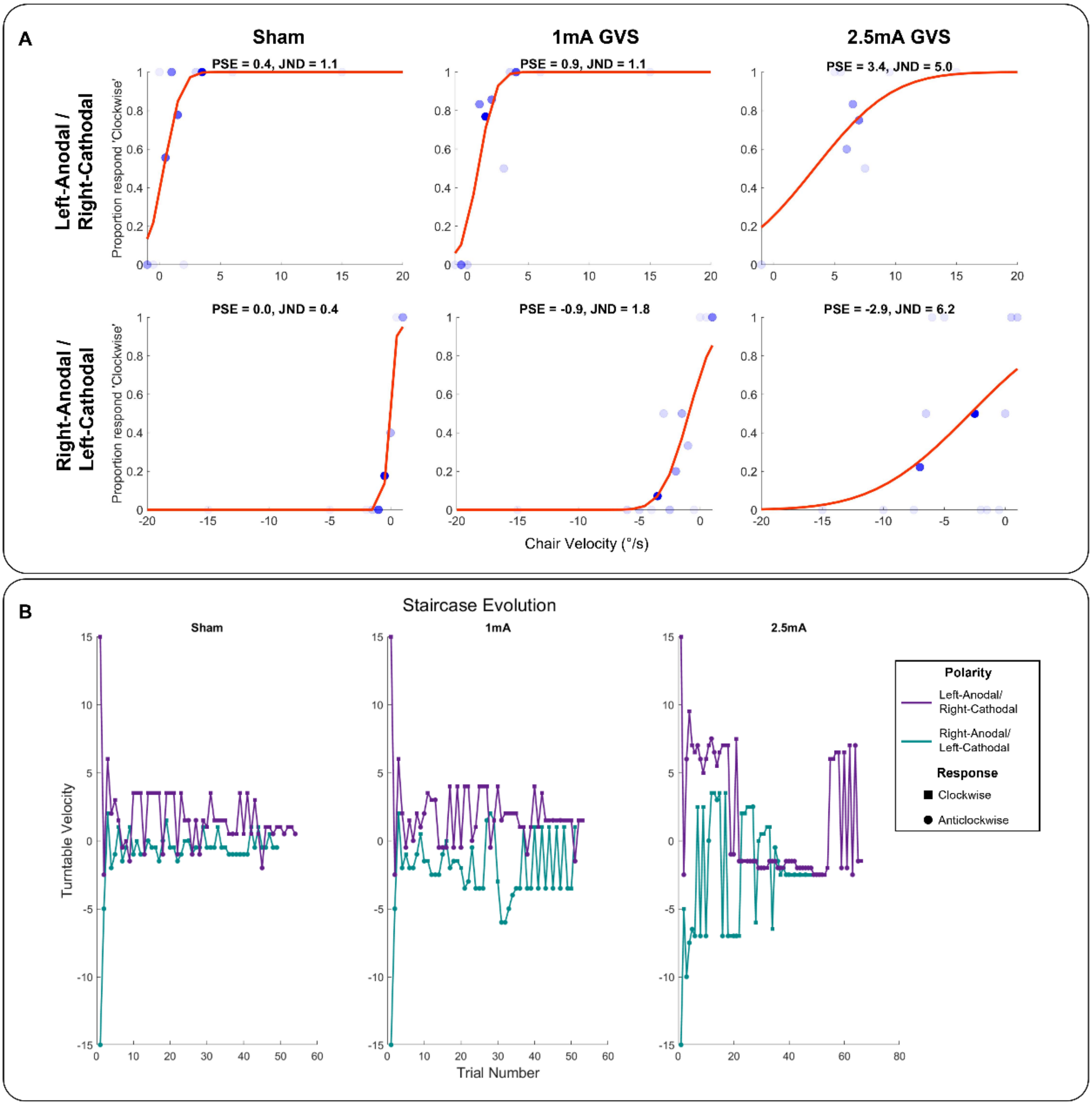
A
Sham
1mA GVS
2.5mA GVS
Left-Anodal / Right-Cathodal
Right-Anodal / Left-Cathodal
Proportion respond 'Clockwise'
PSE = 0.4, JND = 1.1
PSE = 0.9, JND = 1.1
PSE = 3.4, JND = 5.0
PSE = 0.0, JND = 0.4
PSE = -0.9, JND = 1.8
PSE = -2.9, JND = 6.2
Chair Velocity (°/s)
B
Staircase Evolution
Sham
1mA
2.5mA
Turntable Velocity
Trial Number
Polarity
Left-Anodal/ Right-Cathodal
Right-Anodal/ Left-Cathodal
Response
Clockwise
Anticlockwise